Bioorganic Chemistry 109 (2021) 104703

Contents lists available at ScienceDirect

Bioorganic Chemistry

journal homepage: www.elsevier.com/locate/bioorg

Quinazolinone-dihydropyrano[3,2-*b*]pyran hybrids as new α-glucosidase inhibitors: Design, synthesis, enzymatic inhibition, docking study and prediction of pharmacokinetic

Maedeh Sherafati [a], Roghieh Mirzazadeh [b], Ebrahim Barzegari [c], Maryam Mohammadi-Khanaposhtani [d], Homa Azizian [e], Mohammad Sadegh Asgari [f], Samanesadat Hosseini [g], Ebrahim Zabihi [d], Somayeh Mojtabavi [h], Mohammad Ali Faramarzi [h], Mohammad Mahdavi [a,*], Bagher Larijani [a], Hossein Rastegar [i], Haleh Hamedifar [j], Mir Hamed Hajimiri [k,*]

[a] Endocrinology and Metabolism Research Center, Endocrinology and Metabolism Clinical Sciences Institute, Tehran University of Medical Sciences, Tehran, Iran
[b] Department of Biochemistry, Pasteur Institute of Iran, Tehran, Iran
[c] Medical Biology Research Center, Health Technology Institute, Kermanshah University of Medical Sciences, Kermanshah, Iran
[d] Cellular and Molecular Biology Research Center, Health Research Institute, Babol University of Medical Sciences, Babol, Iran
[e] Department of Medicinal Chemistry, School of Pharmacy, Iran University of Medical Sciences, Tehran, Iran
[f] Department of Chemistry, Iran University of Science and Technology, Tehran, Iran
[g] Department of Pharmaceutical Chemistry, School of Pharmacy, Shahid Beheshti University of Medical Sciences, Tehran, Iran
[h] Department of Pharmaceutical Biotechnology, Faculty of Pharmacy, Tehran University of Medical Sciences, Tehran, Iran
[i] Cosmetic Products Research Center, Iranian Food and Drug Administration, MOHE, Tehran, Iran
[j] CinnaGen Medical Biotechnology Research Center, Alborz University of Medical Sciences, Karaj, Iran
[k] Nano Alvand Company, Avicenna Tech Park, Tehran University of Medical Sciences, Tehran, Iran

ARTICLE INFO

Keywords:
α-Glucosidase
Quinazolinone-dihydropyrano[3,2-b]pyran hybrids
α-Amylase
Type 2 diabetes
Docking study
Pharmacokinetic prediction

ABSTRACT

A series of new quinazolinone-dihydropyrano[3,2-*b*]pyran derivatives **10A-L** were synthesized by simple chemical reactions and were investigated for inhibitory activities against α-glucosidase and α-amylase. New synthesized compounds showed high α-glucosidase inhibition effects in comparison to the standard drug acarbose and were inactive against α-amylase. Among them, the most potent compound was compound **10L** (IC_{50} value = 40.1 ± 0.6 μM) with inhibitory activity around 18.75-fold more than acarboase (IC_{50} value = 750.0 ± 12.5 μM). This compound was a competitive inhibitor into α-glucosidase. Our obtained experimental results were confirmed by docking studies. Furthermore, the cytotoxicity of the most potent compounds **10L**, **10G**, and **10N** against normal fibroblast cells and *in silico* druglikeness, ADME, and toxicity prediction of these compounds were also evaluated.

1. Introduction

Diabetes mellitus (DM) is a chronic metabolic disorders with significant prevalence [1]. DM is characterized by hyperglycemia caused by less insulin action or secretion or both [2]. This chronic hyperglycemia leads to microvascular complications in the kidneys, nerves, eyes, and heart [3]. Therefore, blood sugar level control in this disease is the most important goal of treatment [4]. One of the important approaches to lowering blood sugar in non-insulin dependent diabetes (type 2 diabetes) is to inhibit the enzymes that break down large sugars into small sugars [5]. This method helps to reduce the entry of food-related glucose into the bloodstream [6]. The most important target enzymes in this treatment method are α-amylase and α-glucosidase which are found in the digestive system [7]. α-Amylase converted polysaccharides such as starch to oligosaccharides and disaccharides and α-glucosidase converted two latter types of saccharides to monosaccharides such as glucose [8]. Therefore, by inhibiting these enzymes, particularly α-glucosidase, blood glucose level can be reduced [9]. Acarbose, as one

* Corresponding authors.
E-mail addresses: momahdavi@tums.ac.ir (M. Mahdavi), h.hajimiri@nanoalvand.com (M. Hamed Hajimiri).

https://doi.org/10.1016/j.bioorg.2021.104703
Received 30 July 2020; Received in revised form 29 December 2020; Accepted 28 January 2021
Available online 8 February 2021

of the most widely used anti-diabetic drugs, is a potent inhibitor against α-amylase and α-glucosidase [10]. The use of this drug is associated with gastrointestinal side effects that it seems to be due to inhibition of α-amylase because inhibition of this enzyme led to increase undigested starch secretion into the large intestine [11,12]. On the other hand, it is well documented that inhibition of α-glucosidase also is an effective target for treatment of other carbohydrate-related diseases because this enzyme is involved in biosynthesis of glycoproteins in addition to digestion of carbohydrates [13–15]. Thus, access to new and safe α-glucosidase inhibitors is an attractive target for pharmaceutical scientists.

Quinazolinone and its derivatives are found in various biological active agents with anticancer, anti-diabetic, anti-cholinesterase, anti-dihydrofolate reductase, anti-inflammatory, and antimicrobial activities [16–22]. Furthermore, several quinazolinone derivatives with high anti- α-glucosidase inhibitory activity have been reported [23–25]. In this regards, recently, our research group have been presented a new series of quinazolinone-1,2,3-triazole hybrids **A** as potent α-glucosidase inhibitors (Fig. 1, IC_{50} values for compounds **A** = 181.0–474.5 μM comparing with acarbose, 750.0 μM) [26]. On the other hand, pyran-4-one (Fig. 1, compound **B**, IC_{50} value = 34.9 μM) and pyran (Fig. 1, compounds **C** with IC_{50} values = 54.2 μM to not active comparing with acarbose, 937 ± 1.6 μM and compounds **D** with IC_{50} values = 10.3–172.5 μM comparing with acarbose, 750.0 μM) scaffolds were found in the potent α-glucosidase inhibitors **B-D** (Fig. 1) [27–29].

According to the above mentioned-points, in continuation of our previous works about design and synthesis of new hybrid scaffolds with high inhibitory activity into α-glucosidase, herein, we presented a series of quinazolinone-dihydropyrano[3,2-*b*]pyran hybrids as novel agents against α-glucosidase [30–32]. α-Amylase inhibitory activitiy and *in silico* docking and pharmacokinetic studies of these compounds were also performed.

2. Results and discussion

2.1. Chemistry

Synthesis of target quinazolinone-dihydropyrano[3,2-*b*]pyran derivatives **10A-O** was performed according to the starting materials and conditions shown in Scheme 1. As can be seen in this sheme, benzamide derivatives **3** were obtained by the reaction of isatoic anhydride **1** and amine derivatives **2** in water at room temperature. Then, reaction of benzamides **3** and carbon disulfide in the presence of potassium hydroxide in ethanol at reflux condition gave the corresponding thioxo-quinazolinone derivatives **4**. On the other hand, 5-hydroxy-2-(hydroxymethyl)-4H-pyran-4-one **5** in thionyl chloride at room temperature converted to 2-(chloromethyl)-5-hydroxy-4H-pyran-4-one **6**. The latter compound, various benzaldehyde derivatives **7**, and malononitrile **8** in the presence of triethylamine in ethanol at room temperature afforded 2-amino-6-(chloromethyl)-8-oxo-4-phenyl-4,8-dihydropyrano[3,2-*b*] pyran-3-carbonitrile derivatives **9**. Finally, reaction between thioxo-quinazolinones **4** and compounds **9** in the presence of potassium carbonate in DMF provided the title compounds **10A-O**.

2.2. In vitro α-glucosidase and α-amylase inhibitory activities

Synthesized quinazolinone-dihydropyrano[3,2-*b*]pyran derivatives **10A-L** were evaluated against α-glucosidase and α-amylase. Anti-α-glucosidase assay reveled that compounds **10A-L** with IC_{50} values ≤ 142.4 ± 1.9 μM significantly were more potent than standard inhibitor acarbose with IC_{50} value = 750.0 ± 12.5 μM. In contrast, these compounds were inactive (IC_{50} values > 200 μM) against α-amylase in comparison to acarbose (IC_{50} value = 108 ± 0.71 μM).

2.3. Structure-activity relationship (SAR)

In order to better evaluate SAR of the synthesized compounds **10A-O**, these compounds were divided into two categories: aniline

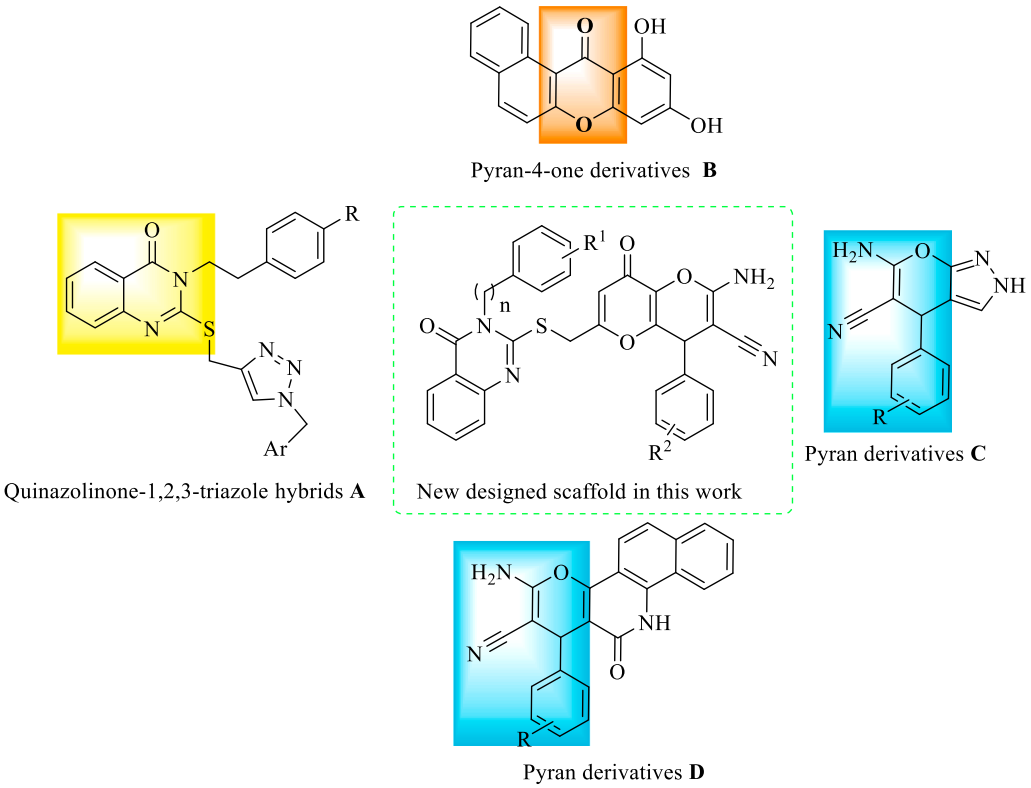

Fig. 1. Rational for the design of quinazolinone-dihydropyrano[3,2-*b*]pyran hybrids as new α-glucosidase inhibitors.

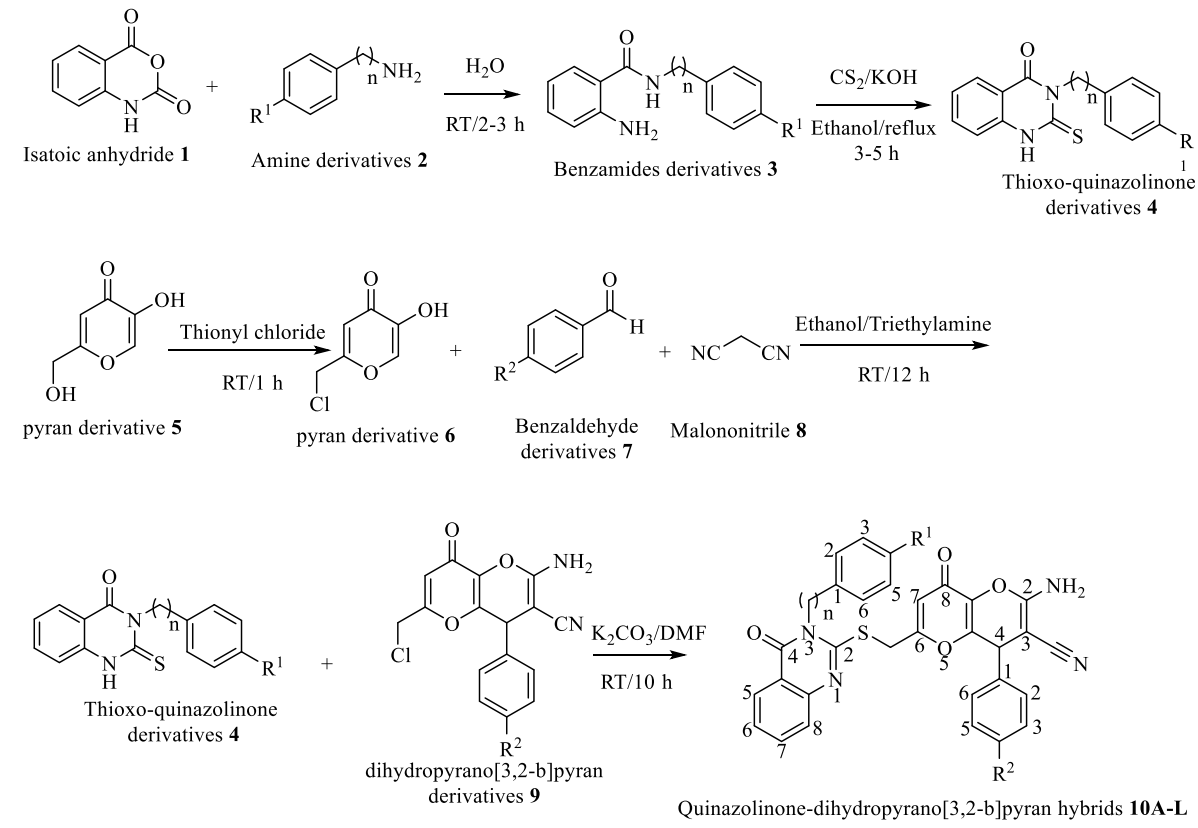

Scheme 1. Synthesis of quinazolinone-dihydropyrano[3,2-*b*]pyran derivatives **10A-L**.

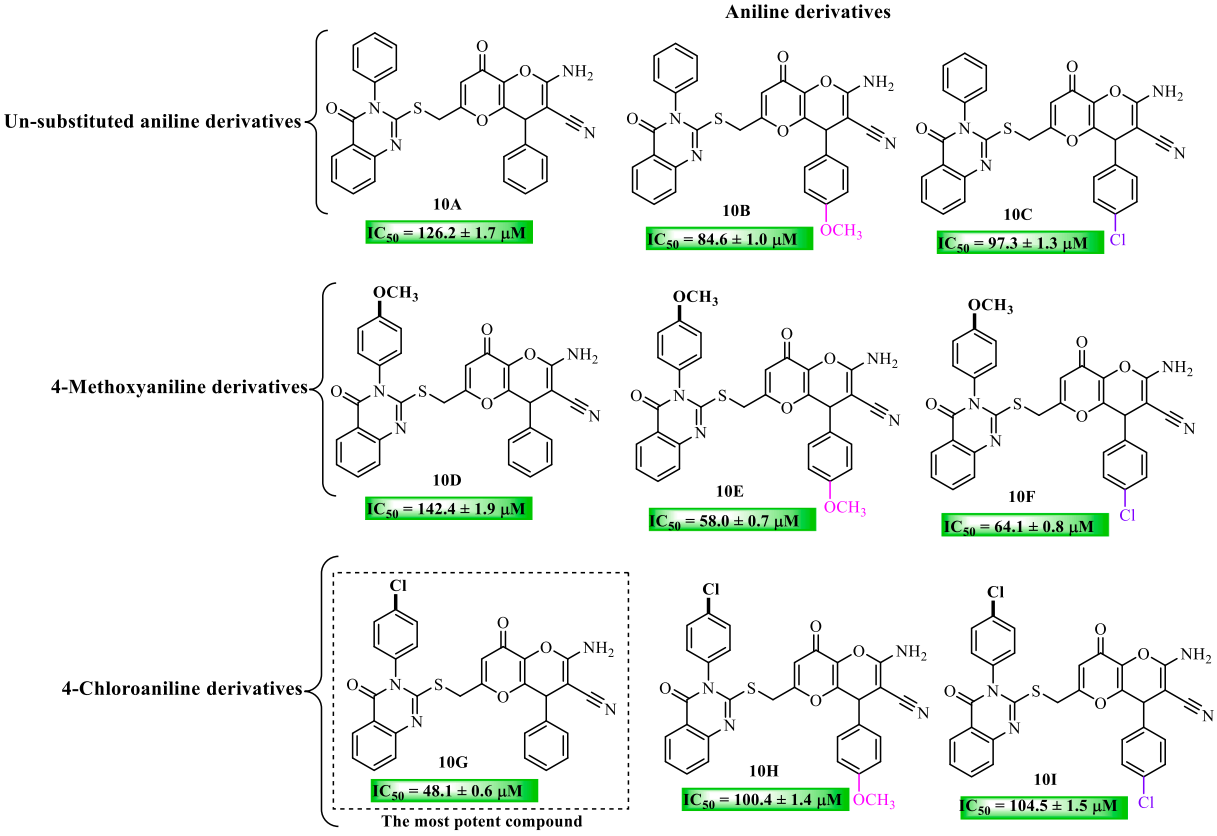

Fig. 2. α-Glucosidase inhibitory activity of aniline derivatives **10A-I.**

derivatives **10A-I** and benzylamine derivatives **10J-O**.

As can be seen in Fig. 2, in the first category, there are three series of aniline derivatives: un-substituted aniline derivatives **10A-C**, 4-methoxyaniline derivatives **10D-F**, 4-chloroaniline derivatives **10G-H**. In each series, substituents on 4-position of pendant phenyl ring of dihydropyrano[3,2-*b*]pyran moiety was altered to optimize anti-α-glucosidase activity.

The most potent compound among the aniline derivatives **10A-I** was 4-chloroaniline derivative **10G** with un-substituted pendant phenyl ring on dihydropyrano[3,2-*b*]pyran moiety. Introduction of methoxy group as electron donating substituent and or chlorine atom as electron withdrawing substituent on 4-position of pendant phenyl ring of dihydropyrano[3,2-*b*]pyran moiety, led to a similar significant 2-fold decrease in inhibitory activity as observed in compounds **10H** and **10I**, respectively. The second most potent compound among the aniline derivatives **10A-I**, was 4-methoxyaniline derivative **10E**. This compound has another methoxy substituent on 4-position of pendant phenyl ring of dihydropyrano[3,2-*b*]pyran ring. Replacement of the latter methoxy group with chlorine atom created a negligible decrease in inhibitory activity while elimination of methoxy group led to significant decrease in activity.

In the un-substituted aniline series **10A-C**, inhibitory activities of the 4-methoxy and 4-chloro derivatives are similar while lack of the substituent on dihydropyrano[3,2-*b*]pyran moiety leads to a significant decrease in inhibitory activity (compounds **10B** and **10C** vs. compound **10A**).

The comparison of IC_{50} values of un-substituted aniline derivative with their corresponding analogs of 4-methoxyaniline and 4-chloroaniline series against α-glucosidase demonstrated that 4-chloroaniline derivative **10G** significantly was more potent than their un-substituted aniline derivative **10A** and 4-methoxyaniline derivative **10D**. On the other hand, 4-methoxyaninline derivatives **10E** and **10F** were more active than their un-substituted aniline analogs **10B** and **10C** and 4-chloroaniline analogs **10H** and **10I**.

Benzylamine category (compounds **10J-O**) can also be divided into two series: un-substituted benzylamine derivatives **10J-L** and 4-fluorobenzylamine derivatives **10M–O** (Fig. 3). In the benzylamine category and among all the synthesized compounds, the most potent compound was compound **10L** of un-substituted benzylamine series. This compound has a chloro substituent on 4-position of dihydropyrano[3,2-*b*]pyran moiety. Replacement of the 4-chloro substituent with methoxy group and or elimination of chlorine atom led to a significant decrease in inhibitory activity. In the 4-fluorobenzylamine derivatives **10M-O**, compound **10N** with 4-methoxy group on dihydropyrano[3,2-*b*]pyran moiety was more potent than their analogs in this series.

Anti-α-glucosidase activity of un-substituted benzylamine derivatives **10J-L** and their corresponding analogs of 4-fluorobenzylamine derivatives **10M-O** demonstrated that with the exception of 4-fluorobenzylamine derivative **10N** (with 4-methoxy substituent on dihydropyrano[3,2-*b*]pyran moiety), un-substituted benzylamine derivatives were more potent of their 4-fluorobenzylamine analogs (compounds **10J** vs. **10M** and compounds **10L** vs. **10O**).

2.4. Kinetic study

The mechanism of activity of the most potent compound **10L** against α-glucosidase was determined by building the Lineweaver–Burk double reciprocal plots and secondary re-plot of the latter plots at increasing concentrations of inhibitor and substrate. Results of the Lineweaver-Burke plots are showed in Fig. 4. These data demonstrated that with increasing inhibitor concentration, Michaelis constant (K_m) values increased while the maximum velocity of reaction (V_{max}) values for this compound did not change. Unchanged V_{max} and increasing K_m values are indicative of competitive mode for inhibition (Fig. 4a). Calculated K_i value for compound **10L** is 38 μM (Fig. 4b).

2.5. Docking study

To evaluate the interaction modes of the new synthesized compounds in the active site of α-glucosidase, docking study was performed using by Auto Dock Tools (version1.5.6). Since in the bioassay, *Saccharomyces cerevisiae* α-glucosidase was used and there was not any X-ray crystallographic structure of this form of enzyme, modeled form of it was constructed by SWISS-MODEL Repository [30]. Then, acarbose as standard α-glucosidase inhibitor and the most potent compounds **10L**, **10G**, and **10N** were docked in the active site of modeled enzyme. The superposed structure of acarbose and the most active compound **10L** and 3D structures of the studied compounds **10L**, **10G**, and **10N** in the active site of α-glucosidase were shown in Fig. 5a-d.

The interaction mode details of acarbose and the most potent synthesized compounds are showed in Fig. 6. As can be seen in this figure, acarbose formed eight hydrogen bonds with active site residues Asn241, Thr301, Ser308, Arg312, Glu304, Thr307, Pro309, and Gln322. This drug also created a hydrophobic interaction with His279 in the active site. Acarbose also established two non-classical hydrogen bonds with His239 and Val305 and two unfavorable interactions with Thr307 and Arg312. Binding energy (BE) of this drug in the α-glucosidase active site was −4.04 kcal/mol.

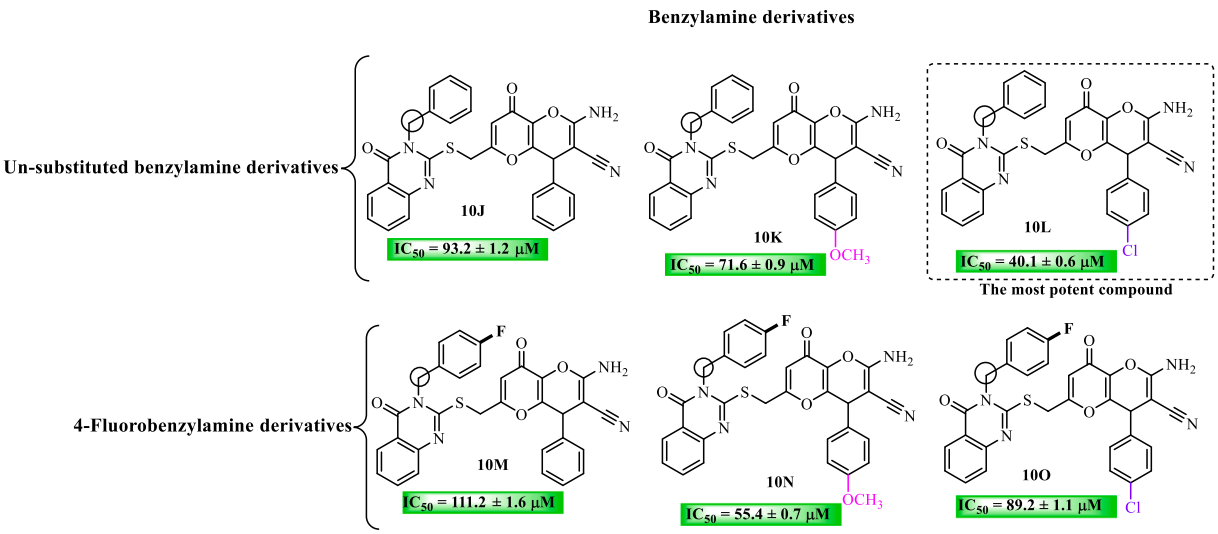

Fig. 3. α-Glucosidase inhibitory activity of benzylamine derivatives **10J-O**.

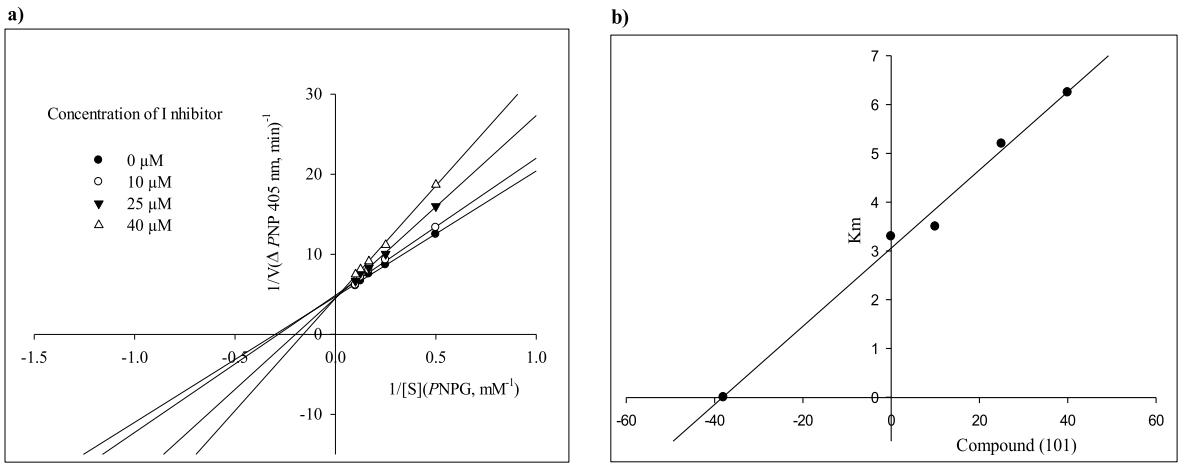

Fig. 4. Kinetic study of α-glucosidase inhibition by compound **10L**. (a) The Lineweaver– Burk plot in the absence and presence of different concentrations of compound **10L**; (b) The secondary plot between K_m and various concentrations of compound **10L**.

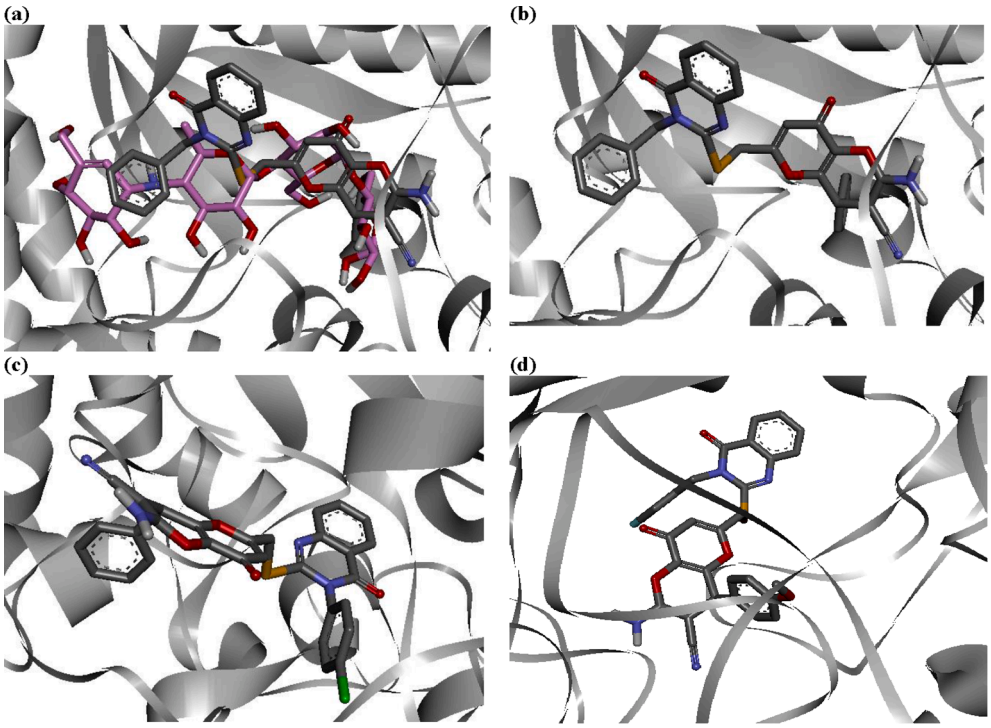

Fig. 5. (a) Superposed structure of acarbose (pink) and the most potent compound **10L**; (b-d) 3D structures of compounds **10L**, **10G**, and **10N**, respectively. (For interpretation of the references to colour in this figure legend, the reader is referred to the web version of this article.)

The most active compound **10L** established three hydrogen bonds with Asn241, His239, and Ser156 *via* carbonyl unit and NH_2 group of dihydropyrano[3,2-*b*]pyran moiety. Pendant phenyl group of the latter moiety created the fallowing interactions: a non-classical hydrogen bond between 4-chloro substituent and Arg439, a π-anion interaction between phenyl group and Asp408, and a hydrophobic interaction between this phenyl ring and Arg312. Quinazolinone moiety of compound **10L** only two interaction formed with active site: a hydrophobic interaction with Pro309 through benzyl moiety and a non-classical hydrogen bond with Asn241 through quinazolinone ring.

Dihydropyrano[3,2-*b*]pyran moiety of the second most potent compound **10G** established a hydrogen bond with Asn241 and a hydrophobic interaction with Arg312 through carbonyl unit and pendant phenyl ring (Fig. 6). Quinazolinone moiety of this compound formed several interactions with active site residues: four hydrophobic interactions with Arg312, Lys155, and Phe311 and a non-classical hydrogen bond with His239.

The third most active compound **10N**, like to compound **10L**, established three hydrogen bonds with Asn241, His239, and Ser156 *via* dihydropyrano[3,2-*b*]pyran moiety while the pendant 4-methoxyphenyl ring of the latter moiety in compound **10N**, unlike compound **10L**, only a hydrophobic interaction formed with active site (Arg312) (Fig. 6). Quinazolinone moiety of compound **10n** formed three π-interactions with His279 and His239.

Calculation of BE of acarbose and the selected compounds predicted that new compounds **10L**, **10G**, and **10N** (BE < -11.00 kcal/mol) with lower BEs in comparison with standard inhibitor (BE = -4.04 kcal/mol) attached to modeled α-glucosidase active site. These findings are in agreement with *in vitro* α-glucosidase inhibition assay (Table 1).

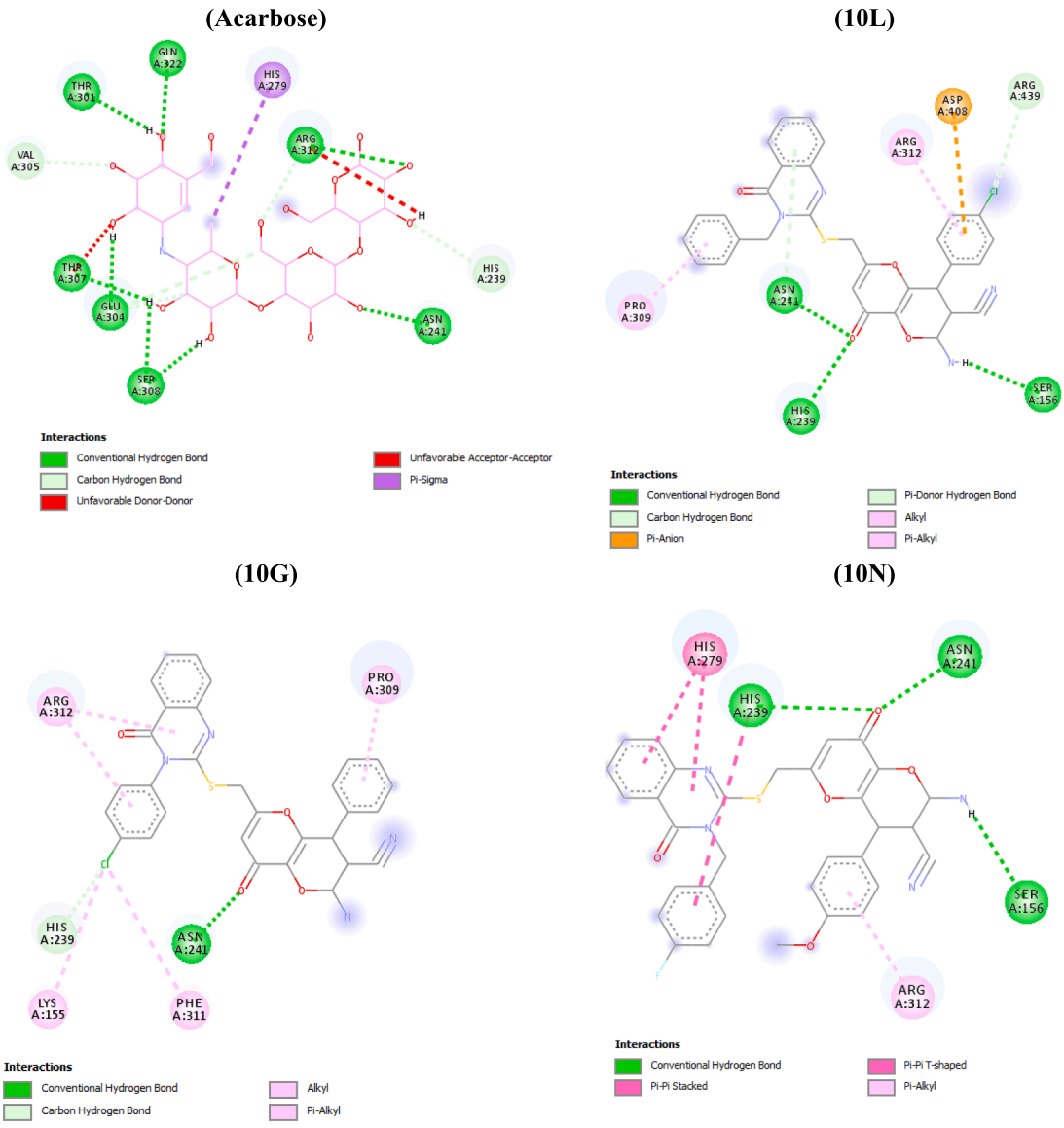

Fig. 6. 2D interaction modes of Acarbose, compounds **10L**, **10G**, and **10N** in the active site of α-glucosidase.

2.6. Cytotoxicity studies

Cytotoxic effects of the compounds **10L**, **10G**, and **10N** as most potent new compounds against α-glucosidase were evaluated against the human normal dermal fibroblasts [33]. Experimental results demonstrated that at 80 μM concentration, all the studied compounds were non-cytotoxic.

2.7. In silico druglikeness, ADME, and toxicity studies

In silico druglikeness/ADME/T properties of the most potent compounds **10L**, **10G**, and **10N** and standard inhibitor acarbose were predicted using by PreADMET as an online software and the obtained results were listed in Table 2 [34]. As can be seen in Table 2, compounds **10L**, **10G**, and **10N** followed of Lipinski 'Rule of five' while acarbose did not follow in this rule. Compounds **10L**, **10G**, and **10N**, and acarbose have poor permeability to Caco-2 cell, blood brain barrier (BBB), and skin. Furthermore, compounds **10L**, **10G**, and **10N** had high human intestinal absorption (HIA) while acarbose did not have HIA. Predicting the toxicity of compounds **10L**, **10G**, and **10N**, and acarbose by PreADMET toxicity server demonstrated that toxicity profile of our new synthesized compounds was similar to acarbose: all the studied compounds were mutagenic and cardiotoxicity (hERG inhibition) of them was ambiguous. Moreover, compounds **10L**, **10G**, and **10N**, like acarbose, presumably did not have carcinogenic effect on rat while may have carcinogenic effect on mouse.

3. Conclusion

In conclusion, we have reported synthesis and biological evaluation of a new series of quinazolinone-dihydropyrano[3,2-*b*]pyran derivatives **10A-O** as new anti-diabetic agents with α-glucosidase inhibition mechanism. These new compounds exhibited excellent α-glucosidase inhibitory activity in comparison to standard inhibitor (acarbose) against yeast α-glucosidase. Among the synthesized compounds, the most potent compounds **10L**, **10G**, and **10N** were selected for further evaluations. Compounds **10L**, **10G**, and **10N** interacted to important residues in the α-glucosidase's active site with less binding energies compared to acarbose. None of the selected compounds showed the cytotoxic effect against normal cells. Druglikeness/ADME/Toxicity prediction of compounds **10L**, **10G**, and **10N** were also performed and compared to acarbose.

Table 1
In vitro α-glucosidase and α-amylase inhibitory activities of compounds **10A-L**.

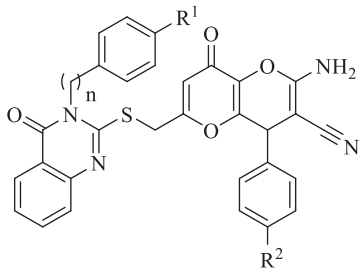

Compound	n	R^1	R^2	IC_{50} (μM)	
				α-Glucosidase	α-Amylase
10A	0	H	H	126.2 ± 1.7	> 200
10B	0	H	OCH_3	84.6 ± 1.0	> 200
10C	0	H	Cl	97.3 ± 1.3	> 200
10D	0	OCH_3	H	142.4 ± 1.9	> 200
10E	0	OCH_3	OCH_3	58.0 ± 0.7	> 200
10F	0	OCH_3	Cl	64.1 ± 0.8	> 200
10G	0	Cl	H	48.1 ± 0.6	> 200
10H	0	Cl	OCH_3	100.4 ± 1.4	> 200
10I	0	Cl	Cl	104.5 ± 1.5	> 200
10J	1	H	H	93.2 ± 1.2	> 200
10K	1	H	OCH_3	71.6 ± 0.9	> 200
10L	1	H	Cl	40.1 ± 0.6	> 200
10M	1	F	H	111.2 ± 1.6	> 200
10N	1	F	OCH_3	55.4 ± 0.7	> 200
10O	1	F	Cl	89.2 ± 1.1	> 200
Acarbose	–	–		750.0 ± 12.5	108 ± 0.71

Table 2
Druglikeness/ADME/T profile of the most potent compounds **10L**, **10G**, and **10N** and standard drug acarbose.

Druglikeness/ADME/T [a]	Compound			
	10L	**10G**	**10N**	**Acarbose**
Rule of Five	Suitable	Suitable	Suitable	Violated
Caco2	22.7856	21.4133	27.1173	9.44448
HIA	98.023306	97.868466	99.302197	0.000000
BBB	0.232575	0.27104	0.158865	0.0271005
Skin Permeability	−2.40258	−2.47285	−2.73422	−5.17615
Ames test	Mutagen	Mutagen	Mutagen	Mutagen
hERG inhibition	Ambiguous	Ambiguous	Ambiguous	Ambiguous
Carcino Mouse	Positive	Positive	Positive	Positive
Carcin Rat	Negative	Negative	Negative	Negative

[a] The recommended ranges for Caco2: < 25 poor, > 500 great, HIA: > 80% is high < 25% is poor, BBB = –3.0 – 1.2, and Skin Permeability = –8.0 – –1.0.

4. Experimental

Melting points of Quinazolinone-dihydropyrano[3,2-*b*]pyran derivatives **10A-O** were measured on a Kofler hot stage apparatus. IR spectra and NMR (^{1}H and ^{13}C) of title compounds were obtained by using a Bruker FT-500 and Nicolet Magna FTIR 550 spectrophotometer on KBr disks, respectively. Mass spectra of title compounds **10A-O** were recorded with an Agilent Technology (HP) mass spectrometer (ionization potential of 70 eV). Elemental analysis was performed by an Elementar Analysensystem Heraeus CHN-O-Rapid analyzer mode. Analytical HPLC was performed on Agilent 1290 Infinity II HPLC system. As column, a Zorbax 300SB-C18, 3.5 μm, 4.6 × 150 mm, Agilent, P/N: 863973-902 was used. HPLC purity was measured using the following binary solvent system: 0.1% trifluoroacetic acid (TFA) in HPLC grade water (90%) and 0.1% TFA in acetonitrile (10%) in 5 min, 0.1% TFA in HPLC grade water (50%) and 0.1% TFA in acetonitrile (50%) in 38 min, 0.1% TFA in HPLC grade water (50%) and 0.1% TFA in acetonitrile (50%) in 40 min, 0.1% TFA in HPLC grade water (90%) and 0.1% TFA in acetonitrile (10%) in 35 min, 0.1% TFA in HPLC grade water (90%) and 0.1% TFA in acetonitrile (10%) in 40 min, flow rate 1 mL/min, λ 322 nm. The purity of the synthesized compounds **10a-o** was determined to be > 96%.

*4.1. General procedure for the preparation of benzamide derivatives **3***

A mixture of isatoic anhydride **1** (20 mmol) and amine derivatives **2** (20 mmol) in water (50 mL) was stirred at room temperature for 2–3 h. After completion of the reaction that was checked by TLC, the precipitated products were filtered off affording pure benzamide derivatives **3**.

*4.2. General procedure for the preparation of thioxo-quinazolinones **4***

A mixture of benzamids **3** (2 mmol), potassium hydroxide (2 mmol), and carbon disulfide in EtOH (10 mL) was heated at reflux for 3–5 h. After completion of the reaction (checked by TLC), the reaction mixture was cooled down to room temperature, poured into cold water, and the precipitated products were filtered off and recrystallized from EtOH to give the corresponding thioxo-quinazolinone derivatives **4**.

*4.3. Synthesis of 2-(chloromethyl)-5-hydroxy-4H-pyran-4-one **6***

A mixture of 5-hydroxy-2-(hydroxymethyl)-4H-pyran-4-one **5** (10 mmol) and thionyl chloride (5 mL) was stirred at room temperature for 1 h. After that, the reaction mixture was filtered off and obtained precipitate **6** was purified by recrystallization in petroleum ether.

*4.4. General procedure for the preparation of 2-amino-6-(chloromethyl)-8-oxo-4-phenyl-4,8-dihydropyrano[3,2-b]pyran-3-carbonitriles **9***

A mixture of 2-(chloromethyl)-5-hydroxy-4H-pyran-4-one **6** (2 mmol), benzaldehyde derivatives **7** (2 mmol), malononitrile **8** (2 mmol), and triethylamine (20 mol%) in ethanol (10 mL) was stirred at room temperature for 12 h. Then, precipitated products **9** were filtered off and were entered to the next reaction with no purification.

*4.5. General procedure for the preparation of quinazolinone-dihydropyrano[3,2-b]pyran derivatives **10A-O***

In the final step of preparation of target compounds **10A-O**, a mixture of thioxo-quinazolinone derivatives **4** (1 mmol), compounds **9** (1 mmol), and potassium carbonate (1.2 mmol) in DMF was stirred at room temperature for 10 h. In the end of reaction (checked by TLC), cold water was added to the reaction mixture and obtained participates were filtered and washed with water to give quinazolinone-dihydropyrano [3,2-*b*]pyran derivatives **10A-O**.

*4.5.1. 2-amino-8-oxo-6-(((4-oxo-3-phenyl-3,4-dihydroquinazolin-2-yl) thio)methyl)-4-phenyl-4,8-dihydropyrano[3,2-b]pyran-3-carbonitrile (**10A**)*

White solid; isolated yield: 96%; mp 167–169 °C; IR (KBr, υ): 3402, 3369, 3026, 2224, 1638 cm^{-1}; ^{1}H NMR (301 MHz, DMSO-d_6) δ 8.11 (dd, J = 7.9, 1.2 Hz, 1H), 7.90 – 7.83 (m, 1H), 7.63 – 7.54 (m, 3H), 7.51 (d, J = 8.1 Hz, 1H), 7.43 (d, J = 8.0 Hz, 1H), 7.38 – 7.22 (m, 7H), 7.15 (d, J = 8.2 Hz, 2H), 6.56 (s, 1H, C—H vinyl), 4.77 (s, 1H, CH), 4.28 (AB-quartet, J = 14.7 Hz, 2H, S-CH_2); ^{13}C NMR (76 MHz, DMSO-d_6) δ 169.86, 164.16, 159.68, 155.64, 149.80, 147.35, 141.13, 136.77, 135.89, 135.43, 130.48, 129.97, 129.81, 129.17, 128.19, 128.09, 127.02, 126.52, 120.15, 119.67, 114.67, 55.98, 47.15, 32.79; EI-MS *m/z*: 532; Anal Calcd for $C_{30}H_{20}N_4O_4S$, C, 67.66; H, 3.79; N, 10.52 found: C, 67.61; H, 3.84; N, 10.48.

*4.5.2. 2-amino-4-(4-methoxyphenyl)-8-oxo-6-(((4-oxo-3-phenyl-3,4-dihydroquinazolin-2-yl)thio)methyl)-4,8-dihydropyrano[3,2-b]pyran-3-carbonitrile (**10B**)*

White solid; isolated yield: 88%; mp 219–221 °C; IR (KBr, υ): 3401,

3367, 3026, 2224, 1630 cm^{-1}; ^1H NMR (301 MHz, DMSO-d_6) δ 8.17 – 8.09 (m, 2H), 7.89 – 7.79 (m, 2H), 7.58 (d, J = 2.6 Hz, 2H), 7.45 (d, J = 8.0 Hz, 1H), 7.21 (d, J = 1.8 Hz, 2H), 7.01 (d, J = 2.3 Hz, 2H), 6.76 (s, 2H), 6.51 (s, 1H, C—H vinyl), 4.63 (s, 1H, CH), 4.16 (AB-quartet, J = 15.3 Hz, 2H, S-CH_2). 3.73 (s, 3H, CH3); ^{13}C NMR (76 MHz, DMSO-d_6) δ 169.84, 164.03, 161.34, 161.09, 159.62, 159.18, 155.64, 155.25, 150.07, 147.36, 146.93, 136.55, 135.91, 135.39, 132.99, 129.07, 127.94, 127.12, 120.13, 119.70, 119.27, 114.41, 56.30, 55.48, 47.22, 32.65; EI-MS *m/z*: 562; Anal Calcd for $C_{31}H_{22}N_4O_5S$, C, 66.18; H, 3.94; N, 9.96 found: C, 66.13; H, 3.95; N, 9.97.

4.5.3. 2-amino-4-(4-chlorophenyl)-8-oxo-6-(((4-oxo-3-phenyl-3,4-dihydroquinazolin-2-yl)thio)methyl)-4,8-dihydropyrano[3,2-b]pyran-3-carbonitrile (10C)

White solid; isolated yield: 92%; mp 188–190 °C; IR (KBr, υ): 3404, 3367, 3020, 2225, 1638 cm^{-1}; ^1H NMR (301 MHz, DMSO-d_6) δ 8.11 (dd, J = 7.9, 1.2 Hz, 1H), 7.89 – 7.83 (m, 1H), 7.61 – 7.56 (m, 3H), 7.51 (d, J = 8.2 Hz, 1H), 7.44 (d, J = 8.0 Hz, 1H), 7.38 – 7.34 (m, 2H), 7.31 – 7.26 (m, 4H), 7.23 – 7.19 (m, 2H), 6.57 (s, 1H, C—H vinyl), 4.85 (s, 1H, CH), 4.15 (AB-quartet, J = 16.2 Hz, 2H, S-CH_2); ^{13}C NMR (76 MHz, DMSO-d_6) δ 169.84, 164.12, 161.03, 159.65, 155.66, 149.21, 147.34, 140.07, 136.86, 135.91, 135.39, 132.94, 130.51, 130.09, 129.86, 129.14, 127.13, 126.71, 126.45, 120.10, 119.53, 114.77, 55.63, 47.22, 32.82; EI-MS *m/z*: 566; Anal Calcd for $C_{30}H_{19}ClN_4O_4S$, C, 63.55; H, 3.38; N, 9.88 found: C, 63.51; H, 3.34; N, 9.86.

4.5.4. 2-amino-6-(((3-(4-methoxyphenyl)-4-oxo-3,4-dihydroquinazolin-2-yl)thio)methyl)-8-oxo-4-phenyl-4,8-dihydropyrano[3,2-b]pyran-3-carbonitrile (10D)

White solid; isolated yield: 93%; mp 174–176 °C; IR (KBr, υ): 3408, 3362, 3029, 2223, 1630 cm^{-1}; ^1H NMR (301 MHz, DMSO-d_6) δ 8.13 – 8.05 (m, 1H), 7.88 – 7.79 (m, 1H), 7.51 (t, J = 7.6 Hz, 1H), 7.43 (d, J = 8.1 Hz, 1H), 7.34 – 7.20 (m, 7H), 7.16 (d, J = 6.4 Hz, 2H), 7.09 (d, J = 8.9 Hz, 2H), 6.56 (s, 1H, C—H vinyl), 4.77 (s, 1H, CH), 4.27 (AB-quartet, J = 15.2 Hz, 2H, S-CH_2), 3.86 (s, 3H, CH_3); ^{13}C NMR (76 MHz, DMSO-d_6) δ 169.88, 164.23, 161.28, 160.62, 159.70, 156.35, 149.79, 147.37, 141.14, 136.77, 135.34, 131.03, 129.18, 128.25, 128.10, 127.03, 126.62, 126.48, 120.13, 119.69, 115.12, 114.65, 62.28, 55.99, 45.08, 32.86; EI-MS *m/z*: 562; Anal Calcd for $C_{31}H_{22}N_4O_5S$, C, 66.18; H, 3.94; N, 9.96 found: C, 66.12; H, 3.96; N, 9.90.

4.5.5. 2-amino-4-(4-methoxyphenyl)-6-(((3-(4-methoxyphenyl)-4-oxo-3,4-dihydroquinazolin-2-yl)thio)methyl)-8-oxo-4,8-dihydropyrano[3,2-b]pyran-3-carbonitrile (10E)

White solid; isolated yield: 89%; mp 181–183 °C; IR (KBr, υ): 3404, 3367, 3025, 2229, 1639 cm^{-1}; ^1H NMR (301 MHz, DMSO-d_6) δ 8.11 (dd, J = 7.9, 1.1 Hz, 1H), 7.89 – 7.80 (m, 1H), 7.57 – 7.49 (m, 1H), 7.45 (d, J = 8.1 Hz, 1H), 7.27 – 7.15 (m, 4H), 7.11 – 7.00 (m, 4H), 6.77 (d, J = 8.7 Hz, 2H), 6.53 (s, 1H, C—H vinyl), 4.69 (s, 1H, CH), 4.28 (AB-quartet, J = 15.4 Hz, 2H, , S-CH_2), 3.86 (s, 3H, CH3), 3.74 (s, 3H, CH3); ^{13}C NMR (76 MHz, DMSO-d_6) δ 169.88, 164.24, 161.28, 160.63, 159.52, 159.17, 156.34, 150.03, 147.38, 136.56, 135.31, 133.17, 131.08, 130.97, 129.23, 128.26, 127.04, 126.46, 120.13, 119.71, 115.07, 114.43, 55.96, 55.47, 51.09, 46.74, 32.78; EI-MS *m/z*: 592; Anal Calcd for $C_{32}H_{24}N_4O_6S$, C, 64.85; H, 4.08; N, 9.45 found: C, 64.78; H, 4.12; N, 9.44.

4.5.6. 2-amino-4-(4-chlorophenyl)-6-(((3-(4-methoxyphenyl)-4-oxo-3,4-dihydroquinazolin-2-yl)thio)methyl)-8-oxo-4,8-dihydropyrano[3,2-b]pyran-3-carbonitrile (10F)

White solid; isolated yield: 90%; mp 170–172 °C; IR (KBr, υ): 3407, 3365, 3026, 2228, 1639 cm^{-1}; ^1H NMR (301 MHz, DMSO-d_6) δ 8.11 (d, J = 7.9 Hz, 1H), 7.85 (t, J = 7.7 Hz, 1H), 7.52 (t, J = 7.5 Hz, 1H), 7.43 (d, J = 8.2 Hz, 1H), 7.36 – 7.18 (m, 8H), 7.10 (d, J = 8.8 Hz, 2H), 6.57 (s, 1H, C—H vinyl), 4.86 (s, 1H, CH), 4.27 (s, 2H, S-CH_2), 3.87 (s, 3H, CH_3); ^{13}C NMR (76 MHz, DMSO- d_6) δ 169.84, 164.20, 161.22, 160.64, 159.64, 156.37, 149.20, 147.35, 140.09, 136.87, 135.31, 132.92, 131.09, 130.10, 129.15, 128.26, 127.08, 126.63, 120.10, 119.54, 115.13, 114.76, 55.98, 51.69, 46.42, 32.85; EI-MS *m/z*: 596; Anal Calcd for $C_{31}H_{21}ClN_4O_5S$, C, 62.36; H, 3.55; N, 9.38 found: C, 62.38; H, 3.52; N, 9.34.

4.5.7. 2-amino-6-(((3-(4-chlorophenyl)-4-oxo-3,4-dihydroquinazolin-2-yl)thio)methyl)-8-oxo-4-phenyl-4,8-dihydropyrano[3,2-b]pyran-3-carbonitrile (10G)

White solid; isolated yield: 92%; mp 222–224 °C; IR (KBr, υ): 3407, 3369, 3022, 2220, 1635 cm^{-1}; ^1H NMR (301 MHz, DMSO-d_6) δ 8.10 (d, J = 7.5 Hz, 1H), 7.86 (t, J = 7.2 Hz, 1H), 7.66 (d, J = 8.1 Hz, 2H), 7.52 (t, J = 7.5 Hz, 1H), 7.42 (t, J = 8.5 Hz, 3H), 7.32 – 7.23 (m, 5H), 7.17 (d, J = 6.4 Hz, 2H), 6.57 (s, 1H, C—H vinyl), 4.78 (s, 1H, CH), 4.30 (s, 2H, S-CH_2); ^{13}C NMR (76 MHz, DMSO- d_6) δ 169.88, 163.99, 161.06, 159.69, 155.27, 149.81, 147.32, 141.13, 136.78, 135.49, 135.28, 134.81, 131.88, 130.11, 129.19, 128.11, 127.02, 126.76, 126.54, 120.11, 119.68, 114.72, 55.98, 45.79, 32.83; EI-MS *m/z*: 566; Anal Calcd for $C_{30}H_{19}ClN_4O_4S$, C, 63.55; H, 3.38; N, 9.88 found: C, 63.47; H, 3.34; N, 9.90.

4.5.8. 2-amino-6-(((3-(4-chlorophenyl)-4-oxo-3,4-dihydroquinazolin-2-yl)thio)methyl)-4-(4-methoxyphenyl)-8-oxo-4,8-dihydropyrano[3,2-b]pyran-3-carbonitrile (10H)

White solid; isolated yield: 90%; mp 176–178 °C; IR (KBr, υ): 3401, 3365, 3023, 2224, 1630 cm^{-1}; ^1H NMR (301 MHz, DMSO-d_6) δ 8.11 (dd, J = 7.9, 1.2 Hz, 1H), 7.91 – 7.81 (m, 1H), 7.67 – 7.61 (m, 2H), 7.57 – 7.50 (m, 1H), 7.47 – 7.34 (m, 3H), 7.21 – 7.15 (m, 2H), 7.04 (d, J = 8.7 Hz, 2H), 6.79 (d, J = 8.7 Hz, 2H), 6.54 (s, 1H, C—H vinyl), 4.70 (s, 1H, CH), 4.30 (AB-quarted, J = 15.5 Hz, 2H, S-CH_2), 3.75 (s, 3H, CH3); ^{13}C NMR (76 MHz, DMSO- d_6) δ 169.88, 164.01, 161.05, 159.51, 159.17, 155.26, 150.05, 147.32, 136.58, 135.46, 135.27, 134.83, 133.19, 131.80, 130.07, 129.25, 127.03, 126.78, 126.51, 120.09, 119.70, 114.45, 56.32, 55.50, 46.72, 32.74; EI-MS *m/z*: 596; Anal Calcd for $C_{31}H_{21}ClN_4O_5S$, C, 62.36; H, 3.55; N, 9.38 found: C, 62.33; H, 3.52; N, 9.32.

4.5.9. 2-amino-4-(4-chlorophenyl)-6-(((3-(4-chlorophenyl)-4-oxo-3,4-dihydroquinazolin-2-yl)thio)methyl)-8-oxo-4,8-dihydropyrano[3,2-b]pyran-3-carbonitrile (10I)

White solid; isolated yield: 96%; mp 201–203 °C; IR (KBr, υ): 3408, 3368, 3027, 2220, 1637 cm^{-1}; ^1H NMR (301 MHz, DMSO-d_6) δ 8.11 (dd, J = 7.9, 1.2 Hz, 1H), 7.91 – 7.83 (m, 1H), 7.70 – 7.63 (m, 2H), 7.57 – 7.50 (m, 1H), 7.48 – 7.41 (m, 3H), 7.35 – 7.25 (m, 4H), 7.22 (d, J = 8.5 Hz, 2H), 6.57 (s, 1H, C—H vinyl), 4.86 (s, 1H, CH), 4.29 (AB-quartet, J = 15.4 Hz, 2H, S-CH_2); ^{13}C NMR (76 MHz, DMSO-d_6) δ 169.84, 163.99, 161.01, 159.64, 155.29, 149.22, 147.30, 140.09, 136.88, 135.46, 135.29, 134.84, 132.92, 131.91, 130.12, 129.16, 127.07, 126.77, 126.48, 120.07, 119.53, 114.82, 55.64, 46.47, 32.81; EI-MS *m/z*: 600; Anal Calcd for $C_{30}H_{18}Cl_2N_4O_4S$, C, 59.91; H, 3.02; N, 9.32 found: C, 59.98; H, 3.01; N, 9.32.

4.5.10. 2-amino-6-(((3-benzyl-4-oxo-3,4-dihydroquinazolin-2-yl)thio)methyl)-8-oxo-4-phenyl-4,8-dihydropyrano[3,2-b]pyran-3-carbonitrile (10J)

White solid; isolated yield: 91%; mp 198–200 °C; IR (KBr, υ): 3407, 3367, 3026, 2229, 1639 cm^{-1}; ^1H NMR (301 MHz, DMSO-d_6) δ 8.11 (dd, J = 7.9, 1.2 Hz, 1H), 7.86 (td, J = 8.5, 8.0, 1.5 Hz, 1H), 7.59 – 7.55 (m, 3H), 7.51 (d, J = 8.0 Hz, 1H), 7.44 (d, J = 8.1 Hz, 1H), 7.34 – 7.22 (m, 7H), 7.15 (dd, J = 7.9, 1.5 Hz, 2H), 6.56 (s, 1H, C—H vinyl), 5.40 (AB-quartet, J = 12.5 Hz, 2H, N-CH2-Ph), 4.78 (s, 1H, CH), 4.28 (AB-quartet, J = 15.4 Hz, 2H, S-CH_2); ^{13}C NMR (76 MHz, DMSO-d_6) δ 169.86, 164.16, 161.08, 159.68, 155.64, 149.80, 147.35, 141.13, 136.77, 135.89, 135.43, 130.48, 129.98, 129.81, 129.17, 128.09, 127.02, 126.71, 126.51, 120.14, 119.67, 114.67, 55.98, 48.12, 45.39, 32.79; EI-MS *m/z*: 546; Anal Calcd for $C_{31}H_{22}N_4O_4S$, C, 68.12; H, 4.06; N, 10.25 found: C,

68.17; H, 4.02; N, 10.19.

4.5.11. 2-amino-6-(((3-benzyl-4-oxo-3,4-dihydroquinazolin-2-yl)thio)methyl)-4-(4-methoxyphenyl)-8-oxo-4,8-dihydropyrano[3,2-b]pyran-3-carbonitrile (10K)

White solid; isolated yield: 86%; mp 202–204 °C; IR (KBr, υ): 3400, 3369, 3025, 2221, 1632 cm^{-1}; ^1H NMR (301 MHz, DMSO-d_6) δ 8.12 (dd, J = 7.9, 1.2 Hz, 1H), 7.90 – 7.81 (m, 1H), 7.59 – 7.50 (m, 4H), 7.45 (d, J = 8.0 Hz, 1H), 7.36 – 7.26 (m, 2H), 7.20 (s, 2H), 7.03 (d, J = 8.7 Hz, 2H), 6.77 (d, J = 8.7 Hz, 2H), 6.53 (s, 1H, C—H vinyl), 5.40 (AB-quartet, J = 12.6 Hz, 2H, N-CH2-Ph), 4.69 (s, 1H, CH), 4.29 (AB-quartet, J = 15.3 Hz, 2H, S-CH_2), 3.74 (s, 3H, CH3); ^{13}C NMR (76 MHz, DMSO-d_6) δ 169.89, 164.17, 161.09, 159.53, 159.18, 155.63, 150.04, 147.36, 136.56, 135.91, 135.39, 133.16, 130.50, 129.94, 129.85, 129.22, 127.03, 126.72, 126.49, 120.12, 119.72, 114.43, 56.29, 55.47, 48.49, 44.99, 32.73; EI-MS m/z: 576; Anal Calcd for $C_{32}H_{24}N_4O_5S$, C, 66.65; H, 4.20; N, 9.72 found: C, 66.59; H, 4.13; N, 9.66.

4.5.12. 2-amino-6-(((3-benzyl-4-oxo-3,4-dihydroquinazolin-2-yl)thio)methyl)-4-(4-chlorophenyl)-8-oxo-4,8-dihydropyrano[3,2-b]pyran-3-carbonitrile (10L)

White solid; isolated yield: 89%; mp 165–167 °C; IR (KBr, υ): 3401, 3360, 3028, 2221, 1631 cm^{-1}; ^1H NMR (301 MHz, DMSO-d_6) δ 8.11 (dd, J = 7.9, 1.2 Hz, 1H), 7.90 – 7.82 (m, 1H), 7.60 – 7.56 (m, 3H), 7.52 (d, J = 8.0 Hz, 1H), 7.44 (d, J = 8.0 Hz, 1H), 7.39 – 7.33 (m, 2H), 7.34 – 7.30 (m, 1H), 7.30 – 7.25 (m, 3H), 7.21 (d, J = 8.5 Hz, 2H), 6.56 (s, 1H, C—H vinyl), 5.40 (AB-quartet, J = 12.6 Hz, 2H, N-CH_2-Ph), 4.85 (s, 1H, CH), 4.29 (s, 2H, S-CH_2); ^{13}C NMR (76 MHz, DMSO- d_6) δ 169.84, 164.12, 161.03, 159.64, 155.67, 149.21, 147.34, 140.07, 136.86, 135.91, 135.39, 132.93, 130.51, 130.09, 129.82, 129.14, 127.07, 126.72, 126.45, 120.10, 119.53, 114.76, 55.63, 48.79, 45.58, 32.82; EI-MS m/z: 580; Anal Calcd for $C_{31}H_{21}ClN_4O_4S$, C, 64.08; H, 3.64; N, 9.64 found: C, 64.10; H, 3.59; N, 9.58.

4.5.13. 2-amino-6-(((3-(4-fluorobenzyl)-4-oxo-3,4-dihydroquinazolin-2-yl)thio)methyl)-8-oxo-4-phenyl-4,8-dihydropyrano[3,2-b]pyran-3-carbonitrile (10M)

White solid; isolated yield: 94%; mp 230–232 °C; IR (KBr, υ): 3406, 3362, 3025, 2228, 1636 cm^{-1}; ^1H NMR (301 MHz, DMSO-d_6) δ 8.13 (dd, J = 8.0, 1.2 Hz, 1H), 7.86 – 7.78 (m, 1H), 7.55 – 7.47 (m, 1H), 7.36 – 7.10 (m, 12H), 6.54 (s, 1H, C—H vinyl), 5.19 (AB-quartet, J = 17.1 Hz, 2H, N-CH_2-Ph), 4.71 (s, 1H, CH), 4.41 (AB-quartet, J = 15.7 Hz, 2H, S-CH_2); ^{13}C NMR (76 MHz, DMSO-d_6) δ 169.84, 164.02, 163.54, 161.93 (d, J = 243.6 Hz), 161.36, 160.32, 159.72, 155.08, 149.80, 146.89, 141.00, 136.66, 135.44, 132.13, 129.53, 129.42, 129.07, 128.15, 128.05, 127.06, 126.84, 126.40, 119.65, 119.32, 116.02, 115.74, 114.56, 55.83, 49.38, 46.67, 32.68; EI-MS m/z: 564; Anal Calcd for $C_{31}H_{21}FN_4O_4S$, C, 65.95; H, 3.75; N, 9.92 found: C, 65.89; H, 3.73; N, 9.91.

4.5.14. 2-amino-6-(((3-(4-fluorobenzyl)-4-oxo-3,4-dihydroquinazolin-2-yl)thio)methyl)-4-(4-methoxyphenyl)-8-oxo-4,8-dihydropyrano[3,2-b]pyran-3-carbonitrile (10N)

White solid; isolated yield: 94%; mp 184–186 °C; IR (KBr, υ): 3407, 3367, 3021, 2229, 1633 cm^{-1}; ^1H NMR (301 MHz, DMSO-d_6) δ 8.14 (dd, J = 8.0, 1.2 Hz, 1H), 7.86 – 7.76 (m, 1H), 7.52 (t, J = 8.1 Hz, 1H), 7.35 (d, J = 7.9 Hz, 1H), 7.31 – 7.24 (m, 2H), 7.22 – 7.10 (m, 4H), 7.02 (d, J = 8.7 Hz, 2H), 6.74 (d, J = 8.7 Hz, 2H), 6.52 (s, 1H, C—H vinyl), 5.20 (AB-quartet, J = 16.5 Hz, 2H, N-CH2-Ph), 4.64 (s, 1H, CH), 4.42 (AB-quartet, J = 15.1 Hz, 2H, S-CH_2), 3.72 (s, 3H, CH_3); ^{13}C NMR (76 MHz, DMSO-d_6) δ 169.85, 164.01, 162.67 (d, J = 201.7 Hz), 161.34, 159.61, 159.17, 155.09, 150.06, 146.90, 136.45, 135.39, 133.00, 132.10, 129.52, 129.41, 129.18, 127.08, 126.86, 126.40, 119.69, 119.29, 116.01, 115.73, 114.46, 114.38, 56.11, 55.46, 50.69, 46.65, 32.66; EI-MS m/z: 594; Anal Calcd for $C_{32}H_{23}FN_4O_5S$, C, 64.64; H, 3.90; N, 9.42 found: C, 64.66; H, 3.99; N, 9.40.

4.5.15. 2-amino-4-(4-chlorophenyl)-6-(((3-(4-fluorobenzyl)-4-oxo-3,4-dihydroquinazolin-2-yl)thio)methyl)-8-oxo-4,8-dihydropyrano[3,2-b]pyran-3-carbonitrile (10O)

White solid; isolated yield: 94%; mp 226–228 °C; IR (KBr, υ): 3408, 3368, 3020, 2221, 1635 cm^{-1}; ^1H NMR (301 MHz, DMSO-d_6) δ 8.14 (dd, J = 8.0, 1.2 Hz, 1H), 7.86 – 7.77 (m, 1H), 7.55 – 7.48 (m, 1H), 7.34 – 7.22 (m, 7H), 7.21 – 7.12 (m, 4H), 6.54 (s, 1H, C—H vinyl), 5.22 (AB-quartet, J = 17.1 Hz, 2H, N-CH2-Ph), 4.79 (s, 1H, CH), 4.41 (s, 2H, S-CH_2); ^{13}C NMR (76 MHz, DMSO- d_6) δ 169.81, 164.05, 161.95 (d, J = 243.7 Hz), 163.56, 161.29, 160.34, 159.72, 155.08, 149.22, 146.87, 139.96, 136.75, 135.38, 132.96, 132.09, 130.05, 129.53, 129.42, 129.08, 127.12, 126.85, 126.32, 119.52, 119.27, 116.03, 115.75, 114.59, 55.47, 48.76, 46.64, 32.68; EI-MS m/z: 598; Anal Calcd for $C_{31}H_{20}ClFN_4O_4S$, C, 62.16; H, 3.37; N, 9.35 found: C, 62.18; H, 3.36; N, 9.34.

4.6. α-Glucosidase inhibition assay

The α-glucosidase inhibitory effects of quinazolinone-dihydropyrano [3,2-*b*]pyran derivatives **10A-O** were determined by our previously reported method [30]. In this method, 20 μL of test compounds **10A-O** with various concentrations, 20 μL of enzyme solution (α-glucosidase from *Saccharomyces cerevisiae,* EC3.2.1.20, 20 U/mg), and 135 μL of potassium phosphate buffer were added and incubated in the 96-well plate for 10 min at 37 °C. Then, 25 μL of substrate (*p*-nitrophenyl glucopyranoside, 4 mM) was added to each well of the plate and incubation was continued for 20 min at 37 °C. After that, absorbance was measured at 405 nm by spectrophotometer (Gen5, Power wave xs2, BioTek, USA), and IC_{50} value for each test compound was calculated using the nonlinear regression curve (logit method).

4.7. In vitro α-amylase inhibition assay

α-Amylase inhibitory activity of the synthesized compounds **10A-O** was screened based on the colorimetric method, according to described method by Taha et al. [35].

4.8. Kinetic evaluation of α-glucosidase inhibition

A kinetic study was performed for determination of α-glucosidase inhibition mechanism of the synthesized compounds. For this purpose, 20 μL of the most potent compound **10L** with different concentrations (0, 10, 25, and 40 μM) and 20 μL of the enzyme solution (1 U/mL) were incubated for 15 min at 30 °C. Then, the enzymatic reaction was initiated by adding different concentrations of substrate (*p*-nitrophenyl glucopyranoside, 1–4 mM), and change in absorbance was measured for 20 min at 405 nm by using spectrophotometer (Gen5, Power wave xs2, BioTek, America).

4.9. Docking study

Docking study of the most potent compounds **10L**, **10G**, and **10N** in the modeled α-glucosidase active site was performed according to our previously described method [30].

4.10. In vitro cytotoxicity assay

In vitro cytotoxicity assay of compounds **10L**, **10G**, and **10N** was determined by MTT assay in triplicate according to our recently published work [31].

4.11. In silico Druglikeness/ADME/T study

In silico Druglikeness/ADME/T studies of the most potent compounds **10L**, **10G**, and **10N** were performed using the preADMET online server [34].

Declaration of Competing Interest

The authors declare that they have no known competing financial interests or personal relationships that could have appeared to influence the work reported in this paper.

Appendix A. Supplementary material

Supplementary data to this article can be found online at https://doi.org/10.1016/j.bioorg.2021.104703.

References

[1] M. Navasa, J. Bustamante, C. Marroni, E. González, H. Andreu, E. Esmatjes, J. C. García-Valdecasas, L. Grande, I. Cirera, A. Rimola, J. Rodés, Diabetes mellitus after liver transplantation: prevalence and predictive factors, J. Hepatol. 25 (1996) 64–71.

[2] D. Mellitus, Diagnosis and classification of diabetes mellitus, Diabetes care 28 (2005) S5–S10.

[3] M.J. Sheetz, G.L. King, Molecular understanding of hyperglycemia's adverse effects for diabetic complications, Jama 288 (2002) 2579–2588.

[4] M. Laakso, H. Cederberg, Glucose control in diabetes: which target level to aim for? J. Intern. Med. 272 (2012) 1–12.

[5] J.B. Lamine, M.A. Boujbiha, S. Dahane, A.B. Cherifa, A. Khlifi, H. Chahdoura, M. T. Yakoubi, S. Ferchichi, N. El Ayeb, L. Achour, A-amylase and α-glucosidase inhibitor effects and pancreatic response to diabetes mellitus on wistar rats of ephedra alata areal part decoction with immunohistochemical analyses, Environ. Sci. Pollut. Res. 26 (2019) 9739–9754.

[6] D.J. Jenkins, M.J. Thorne, K. Camelon, A. Jenkins, A.V. Rao, R.H. Taylor, L. U. Thompson, J. Kalmusky, R. Reichert, T. Francis, Effect of processing on digestibility and the blood glucose response: a study of lentils, Am. J. Clin. Nutr. 36 (1982) 1093–1101.

[7] S. Chiba, Molecular mechanism in α-glucosidase and glucoamylase, Biosci. Biotechnol. Biochem. 61 (1997) 1233–1239.

[8] R.F. Power, Enzymatic conversion of starch to fermentable sugars, The Alcohol Textbook (2003) 23–32.

[9] D.D. Schmidt, W. Frommer, B. Junge, L. Müller, W. Wingender, E. Truscheit, D. Schäfer, α-Glucosidase inhibitors, Naturwissenschaften 64 (1977) 535–536.

[10] A.E. Martin, P.A. Montgomery, Acarbose: An α-glucosidase inhibitor, Am. J. Health-Syst. Pharm. 53 (1996) 2277–2290.

[11] Y. Dong, B. Zhang, W. Sun, Y. Xing, Intervention of Prediabetes by Flavonoids From Oroxylum indicum, In Bioactive Food as Dietary Interventions for Diabetes: Academic Press (2019) 559-575.

[12] P. Hollander, Safety profile of acarbose, an α-glucosidase inhibitor, Drugs 44 (1992) 47–53.

[13] R. Pili, J. Chang, R.A. Partis, R.A. Mueller, F.J. Chrest, A. Passaniti, The aglucosidase I inhibitor castanospermine alters endothelial cell glycosylation, prevents angiogenesis, and inhibits tumor growth, Cancer Res. 55 (1995) 2920–2926.

[14] E. Fenouillet, J.C. Gluckman, Effect of a glucosidase inhibitor on the bioactivity and immunoreactivity of human immunodeficiency virus type 1 envelope glycoprotein, J. Gen. Virol. 72 (1991) 1919–1926.

[15] Y. Shimada, E. Nishimura, H. Hoshina, H. Kobayashi, T. Higuchi, Y. Eto, H. Ida, T. Ohashi, Proteasome inhibitor bortezomib enhances the activity of multiple mutant forms of lysosomal a-glucosidase in Pompe disease, JIMD Reports 18 (2015) 33–39.

[16] M. Ghasemian, M. Mahdavi, P. Zare, M.A.H. Feizi, Spiroquinazolinone-induced cytotoxicity and apoptosis in K562 human leukemia cells: alteration in expression levels of Bcl-2 and Bax, J. Toxicol. Sci. 40 (2015) 115–126.

[17] M.S. Malamas, J. Millen, Quinazolineacetic acids and related analogs as aldose reductase inhibitors, J. Med. Chem. 34 (1991) 1492–1503.

[18] R. Ujan, A. Saeed, P.A. Channar, F.A. Larik, Q. Abbas, M.F. Alajmi, H.R. El-Seedi, M.A. Rind, M. Hassan, H. Raza, S.Y. Seo, Drug-1, 3, 4-thiadiazole conjugates as novel mixed-type inhibitors of acetylcholinesterase: synthesis, molecular docking, pharmacokinetics, and ADMET evaluation, Molecules 24 (2019) 860.

[19] S.T. Al-Rashood, I.A. Aboldahab, M.N. Nagi, L.A. Abouzeid, A.A. Abdel-Aziz, S. G. Abdel-hamide, K.M. Youssef, A.M. Al-Obaid, H.I. El-Subbagh, Synthesis, dihydrofolate reductase inhibition, antitumor testing, and molecular modeling study of some new 4 (3H)-quinazolinone analogs, Bioorg. Med. Chem. 14 (2006) 8608–8621.

[20] C. Balakumar, P. Lamba, D.P. Kishore, B.L. Narayana, K.V. Rao, K. Rajwinder, A. R. Rao, B. Shireesha, B. Narsaiah, Synthesis, anti-inflammatory evaluation and docking studies of some new fluorinated fused quinazolines, Eur. J. Med. Chem. 45 (2012) 4904–4913.

[21] F. Khajoee Nejad, M. Khosravan, S.Y. Ebrahimipour, F. Bisceglie, A mixed-ligand quinazoline-based Ni (II) Schiff base complex: Synthesis, characterization, crystal structure, antimicrobial investigation and catalytic activity for the synthesis of 2H–indazolo[2,1-b] phthalazine-triones, Appl. Organometal. Chem. 32 (2018), e3907.

[22] A. Gangjee, O.O. Adair, M. Pagley, S.F. Queener, N9-substituted 2, 4-diaminoquinazolines: synthesis and biological evaluation of lipophilic inhibitors of Pneumocystis carinii and Toxoplasma gondii dihydrofolate reductase, J. Med. Chem. 51 (2008) 6195–6200.

[23] K. Javaid, S.M. Saad, S. Rasheed, S.T. Moin, N. Syed, I. Fatima, U. Salar, K.M. Khan, S. Perveen, M.I. Choudhary, 2-Arylquinazolin-4(3H)-ones: a new class of α-glucosidase inhibitors, Bioorg. Med. Chem. 23 (2015) 7417–7421.

[24] V. Gurram, R. Garlapati, C. Thulluri, N. Madala, K.S. Kasani, P.K. Machiraju, R. Doddapalla, U. Addepally, R. Gundla, B. Patro, N. Pottabathini, Design, synthesis, and biological evaluation of quinazoline derivatives as α-glucosidase inhibitors, Med. Chem. Res. 24 (2015) 2227–2237.

[25] M. Wei, W.M. Chai, R. Wang, Q. Yang, Z. Deng, Y. Peng, Quinazolinone derivatives: synthesis and comparison of inhibitory mechanisms on α-glucosidase, Bioorg. Med. Chem. 25 (2017) 1303–1308.

[26] M. Saeedi, M. Mohammadi-Khanaposhtani, P. Pourrabia, N. Razzaghi, R. Ghadimi, S. Imanparast, M.A. Faramarzi, F. Bandarian, E.N. Esfahani, M. Safavi, H. Rastegar, Design and synthesis of novel quinazolinone-1, 2, 3-triazole hybrids as new antidiabetic agents: in vitro α-glucosidase inhibition, kinetic, and docking study, Bioorg. Chem. 83 (2019) 161–169.

[27] Y. Liu, L. Zou, L. Ma, W.H. Chen, B. Wang, Z.L. Xu, Synthesis and pharmacological activities of xanthone derivatives as a-glucosidase inhibitors, Bioorg. Med. Chem. 14 (2006) 5683–5690.

[28] H. Kashtoh, M.T. Muhammad, J.J. Khan, S. Rasheed, A. Khan, S. Perveen, K. Javaid, K.M. Khan, M.I. Choudhary, Dihydropyrano [2,3-c] pyrazole: novel in vitro inhibitors of yeast a-glucosidase, Bioorg. Chem. 65 (2016) 61–72.

[29] H. Nikookar, M. Mohammadi-Khanaposhtani, S. Imanparast, M.A. Faramarzi, P. R. Ranjbar, M. Mahdavi, B. Larijani, Design, synthesis and in vitro α-glucosidase inhibition of novel dihydropyrano [3,2-c]quinoline derivatives as potential antidiabetic agents, Bioorg. Chem. 77 (2018) 280–286.

[30] M. Adib, F. Peytam, M. Rahmanian-Jazi, S. Mahernia, H.R. Bijanzadeh, M. Jahani, M. Mohammadi-Khanaposhtani, S. Imanparast, M.A. Faramarzi, M. Mahdavi, B. Larijani, New 6-amino-pyrido [2,3-d]pyrimidine-2,4-diones as novel agents to treat type 2 diabetes: a simple and efficient synthesis, α-glucosidase inhibition, molecular modeling and kinetic study, Eur. J. Med. Chem. 155 (2018) 353–363.

[31] M.S. Asgari, M. Mohammadi-Khanaposhtani, M. Kiani, P.R. Ranjbar, E. Zabihi, R. Pourbagher, R. Rahimi, M.A. Faramarzi, M. Biglar, B. Larijani, M. Mahdavi, Biscoumarin-1, 2, 3-triazole hybrids as novel anti-diabetic agents: Design, synthesis, in vitro α-glucosidase inhibition, kinetic, and docking studies, Bioorg. Chem. 92 (2019), 103206.

[32] M. Mohammadi-Khanaposhtani, S. Rezaei, R. Khalifeh, S. Imanparast, M. A. Faramarzi, S. Bahadorikhalili, M. Safavi, F. Bandarian, E.N. Esfahani, M. Mahdavi, B. Larijani, Design, synthesis, docking study, α-glucosidase inhibition, and cytotoxic activities of acridine linked to thioacetamides as novel agents in treatment of type 2 diabetes, Bioorg. Chem. 80 (2018) 288–295.

[33] S. Pandamooz, A. Hadipour, H. Akhavan-Niaki, M. Pourghasem, Z. Abedian, A. M. Ardekani, M. Golpour, Z.M. Hassan, A. Mostafazadeh, Short exposure to collagenase and coculture with mouse embryonic pancreas improve human dermal fibroblast culture, Biotechnol. Appl. Biochem. 59 (2012) 254–261.

[34] Seul, South Corea: Bioinformatics and Molecular Design Research Center; 2004. PreADMET program. Available from: URL: http://preadmet.bmdrc.org.

[35] M. Taha, M.S. Baharudin, N.H. Ismail, S. Imran, M.N. Khan, F. Rahim, M. Selvaraj, S. Chigurupati, M. Nawaz, F. Qureshi, S. Vijayabalan, Synthesis, α-amylase inhibitory potential and molecular docking study of indole derivatives, Bioorg. Chem. 80 (2018) 36–42.